Research Paper

Molecular anatomy of the subcellular localization and nuclear import mechanism of herpes simplex virus 1 UL6

Mingsheng Cai[1,*], Xiaowen Ou[1,*], Yiwen Li[1,*], Xingmei Zou[1], Zuo Xu[1], Yuanfang Wang[1], Hao Peng[1], Yangxi Deng[1], Yingjie Guo[1], Manjiao Lu[1], Weidong Gan[1], Tao Peng[2,3], Meili Li[1]

[1]Guangdong Provincial Key Laboratory of Allergy and Clinical Immunology, Second Affiliated Hospital of Guangzhou Medical University, Sino-French Hoffmann Institute, School of Basic Medical Science, Guangzhou Medical University, The Sixth Affiliated Hospital of Guangzhou Medical University, Qingyuan People's Hospital, Guangzhou 510260, Guangdong, China
[2]State Key Laboratory of Respiratory Diseases, Sino-French Hoffmann Institute, School of Basic Medical Science, Guangzhou Medical University, Panyu, Guangzhou 511436, Guangdong, China
[3]South China Vaccine Corporation Limited, Guangzhou Science Park, Guangzhou 510663, Guangdong, China
*Equal contribution and Co-first authors

Correspondence to: Meili Li; **email:** meili_2011@hotmail.com
Keywords: HSV-1, UL6, nuclear import, importin, Ran-GTP
Received: July 12, 2019 **Accepted:** February 8, 2020 **Published:** April 1, 2020

ABSTRACT

As an indispensable structure protein, the herpes simplex virus 1 (HSV-1) UL6 has been described to exert numerous roles in viral proliferation. However, its exact subcellular localization and subcellular transport mechanism is not well known. In the present study, by utilizing confocal fluorescent microscopy, UL6 was shown to mainly locate in the nucleus in enhanced yellow fluorescent protein or Flag tag fused expression plasmid-transfected cells or HSV-1-infected cells, whereas its predicted nuclear localization signal was nonfunctional. In addition, by exploiting dominant negative mutant and inhibitor of different nuclear import receptors, as well as co-immunoprecipitation and RNA interference assays, UL6 was established to interact with importin α1, importin α7 and transportin-1 to mediate its nuclear translocation under the help of Ran-mediated GTP hydrolysis. Accordingly, these results will advance the knowledge of UL6-mediated biological significances in HSV-1 infection cycle.

INTRODUCTION

Herpes simplex virus 1 (HSV-1), a large nuclear duplicating DNA virus, is an epidemic human microbe that can provoke a lytic infection in the mucosal epithelial cells but a life-long latent infection in neurons. As one of the fundamental structure proteins of HSV-1, UL6 has obtained remarkable concern by virtue of its association with numerous viral propagation processes, including establishing the portal for DNA entry into the HSV capsid, cleavage, processing and packaging of replicated viral DNA, assembling of a minor constituent of virions and capsids, and locating on the external surface of the viral capsid [1–6]. Besides, recent studies also showed that the tryptophan residues or putative leucine zipper of UL6 is crucial for its association with scaffold proteins, UL15 and UL28 proteins, as well as the incorporation of the portal into capsids [7–10]. However, the definite function of UL6 is still poorly understood.

As it is known to all, investigating the precise subcellular localization of a specific protein is a meaningful way to initially discern its detailed roles. UL6 has been previously demonstrated to target to the nuclei in chemical fixed cells [1, 4, 11, 12]. By employing the extensively used fluorescent microscopy technique [13–24], here we established that UL6 was principally

localized to the nuclei in both transient transfected live and chemical fixed cells, as well as in HSV-1-infected cells. Furthermore, UL6 was demonstrated to be transported to the nucleus through a Ran-, importin α1-, importin α7- and transportin-1-dependent nuclear import mechanism, which was predominantly mediated by importin α7 and transportin-1.

RESULTS AND DISCUSSION

Subcellular localization of UL6 in the plasmid transfected and virus infected cells

Protein is the executor of life activity, which need to be transported into certain cell compartments for its execution of specific biological function. UL6 was previously demonstrated to localize in the nucleus in chemical fixed cells [1, 4, 11, 12]. To further detect the subcellular distribution of UL6 in plasmid transfected live cells, enhanced yellow fluorescent protein (EYFP)-tagged UL6 and confocal fluorescence microscopy were adapted. Subsequently, plasmid encoding UL6 fused to the C-terminus of EYFP was constructed and transfected into COS-7 cells to test the subcellular localization of UL6, without the presence of other HSV-1 constituents. Although EYFP-UL6 could show cytoplasmic or pan-cellular localization, it largely exhibited nuclear localization (Figure 1A and Table 1). On the contrary, the fluorescence of vector control EYFP was homogeneously dispersed throughout the cytoplasm and the nucleus in cells transfected with pEYFP-C1 (Figure 1B and Table 1).

Since EYFP is a relatively considerable tag (~27 kDa), it may alter the nuclear localization of UL6. To avoid this hypothesis, plasmid encoding Flag-tagged UL6 (pCMV-Flag-UL6) was constructed and immunofluorescence assay (IFA) was performed to examine the subcellular localization of the UL6. As shown in Figure 1C and Table 1, Flag-tagged UL6 also localized in the nucleus following formaldehyde-based fixation method.

It is well known that viral protein may show distinct subcellular localization fashions in plasmid transfected and virus infected cells. Therefore, the subcellular localization of UL6 was investigated in HSV-1 infected cells. For this sake, Vero cells were infected with HSV-1 and then IFA was carried out. As a result, UL6 also displayed dominantly nuclear localization when cells were infected at an MOI of 1 at 8 h post-infection (Figure 1D and Table 1).

Accordingly, the above data showed that UL6 localized in the nucleus regardless in live cells or chemical fixed cells, as well as in plasmid transfected cells or HSV-1 infected cells. UL6 is shown to exert certain roles that are generally associated with the nucleus, such as constituting the portal for the access of DNA into the HSV capsid, installing of a minor constituent of virions and capsids, and cleavage, disposal and encasement of duplicated viral DNA [1–9, 25]. Thus, it is no wonder that UL6 presents primarily nuclear localization.

Identification of the nuclear localization signal of UL6

Nuclear localization signal (NLS), predominantly possessed of basic residues, is vital for the nuclear accumulation of specific protein [26]. Bioinformatics analysis using PSORT II predicted that UL6 contains a potential NLS in the basic residue rich region, namely PILRKRQ at aa171-177 (pat7). However, the potential nuclear export signal of UL6 was not predicted. In order to identify the functional NLS, UL6 was firstly divided into two segments (amino acids (aa) 1-296 and aa297-676) and fused to the C-terminus of EYFP to construct aa1-296-EYFP and aa297-676-EYFP (Figure 2A). Then, these two plasmids were analyzed in COS-7 cells. As shown in Figure 2B and Table 2, the fluorescence of aa1-296-EYFP showed cytoplasmic localization, whereas aa297-676-EYFP showed pan-cellular distribution, suggesting these two regions may not contain functional NLS. To further explore the functional NLS, plasmids encoding EYFP fused to two diverse segments aa1–177 and aa171–296, which encompass the predicted NLS aa171-177, were constructed (Figure 2A) and assessed in COS-7 cells. As shown in Figure 2B and Table 2, both of the fluorescence of aa1–177-EYFP and aa171–296-EYFP were similar to that of aa1-296-EYFP, indicating the predicted NLS was non-functional, and the functional NLS of UL6 may be generated by spatial conformation.

Characterization of the nuclear import mechanism of UL6

To date, Ran GTPase is reported to be indispensable for the nuclear transport process of most nuclear target protein [27]. To probe the nuclear import mechanism of UL6, the dominant negative (DN) mutant of RanGTP, with deficiency in GTP hydrolysis (Ran-Q69L) [28], was utilized to inspect whether Ran participates in the nuclear translocation of UL6. Plasmids expressing Ran-Q69L-mCherry and FLAG-UL6 were co-transfected into COS-7 cells, then their subcellular distributions were analysed by IFA. As a result, co-transfection of Ran-Q69L significantly abolished the nuclear accumulation of UL6 (Figure 3A and Table 3). Considering the evolutionary conserved nuclear pore complex (NPC) only endorses the dispersion of small proteins with approximate molecular masses of 40~60 kDa [29, 30], and FLAG-UL6 has a molecular mass of about 76 kDa, it cannot be proposed to export the

nucleus by simple dispersion. Consequently, UL6 is a Ran-associated protein and is transported into the nucleus from the cytoplasm through a canonical nuclear transport pathway mediated by GTP hydrolysis.

About the nuclear translocation, the NLS of cargo is bound by different members of the importin family. In heterodimer importin α/β, importin α binds the NLS of a specific cargo, while importin β is responsible for the conformational alteration of importin α, to reinforce the interaction of importin α-NLS [31]. Then, the importin α/β-cargo complex traffics into the nucleus and is detached by the combination of importin β1 (karyopherin β1, kβ1) with Ran-GTP [32]. In mammals, the subcellular transport involves at least six cellular transporters [33, 34], namely importin α1 (karyopherin α2, kα2), importin α3 (karyopherin α4, kα4), importin α4 (karyopherin α3, kα3), importin α5 (karyopherin α1, kα1), importin α6 (karyopherin α5, kα5) and importin α7 (karyopherin α6, kα6). Besides, the NLS-containing cargo also can be directly bound by diverse importin β members [35, 36]. To identify the cellular transporter for the nuclear targeting of UL6, the expression plasmids of importin α1, α3, α6 and α7 nuclear transport inhibitor Bimax2 [37], transportin-1 (importin β2) nuclear import inhibitor M9M [38], importin β association deficient mutant of importin α5 (DN kα1) [39] and Ran binding deficient mutant of importin β1 (DN kβ1) were co-transfected with FLAG-UL6 expression plasmid, respectively. As results (Figure 3B and Table 3),

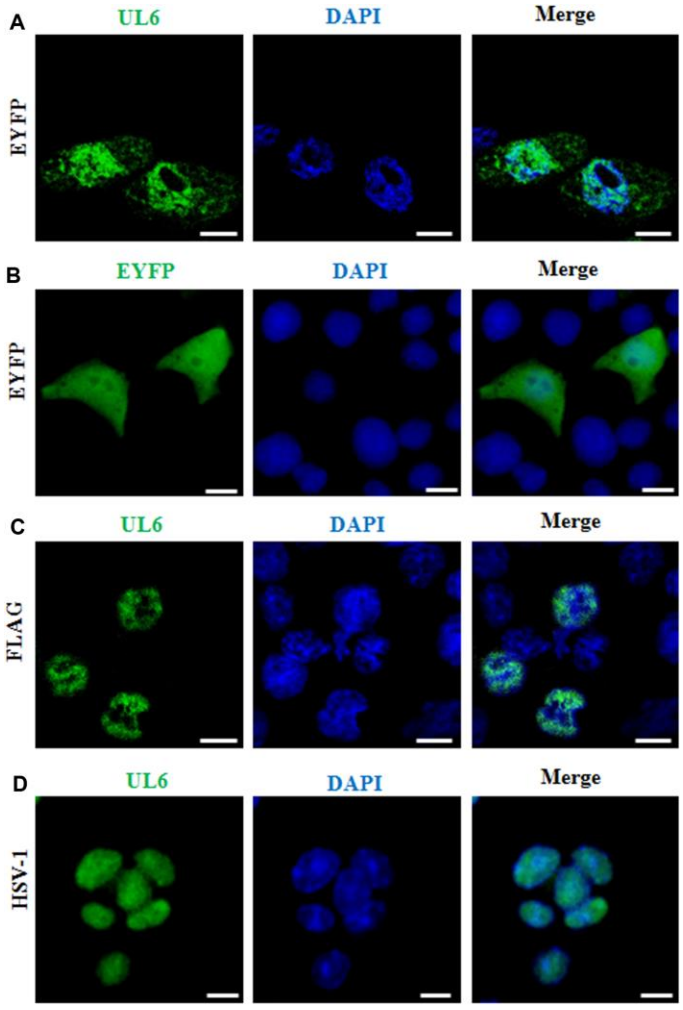

Figure 1. Subcellular distribution of UL6 in plasmid-transfected and HSV-1-infected cells. Subcellular distribution of EYFP-UL6 (**A**), EYFP (**B**) and FLAG-UL6 (**C**) in related plasmid transfected COS-7 cells. (**D**) Subcellular distribution of UL6 in HSV-1 infected Vero cells. Vero cells were infected with HSV-1 (F strain) at an MOI of 1. 8 h post-infection, Vero cells were fixed with 4% paraformaldehyde, permeabilized with 0.5% Triton X-100, and incubated with the anti-UL6 pAb. Then, cells were incubated with FITC-conjugated goat anti-rabbit IgG (green) and stained with DAPI (blue) to visualize the nuclei. EYFP fusion proteins were shown in pseudocolor green. The image shown represents a great proportion of the cells with homogeneous subcellular distribution. All scale bars indicate 10 um. Statistical analysis of the fluorescence was shown in Table 1.

Table 1. Subcellular localization of HSV-1 UL6.

Transfection or infection	Detected protein	Total number of cells transfected with plasmid or infected with virus	Number of cells with predominant nuclear localization	Percentage of cells with predominant nuclear localization
Transfected with EYFP-UL6	UL6	30	21	70
Transfected with EYFP vector	EYFP	30	0	0
Transfected with Flag-UL6	UL6	30	29	96.67
Infected with HSV-1	UL6	30	30	100

COS-7 cells were transfected with plasmid expressing EYFP-UL6 or EYFP for 24 h, then cells were examined by confocal fluorescence microscopy. In addition, COS-7 cells were transfected with plasmid expressing Flag-UL6 for 24 h, and Vero cells were infected with HSV-1 (F strain) at an MOI of 1 for 8 h, then cells were subjected to IFA analysis using anti-Flag mAb or anti-UL6 pAb.

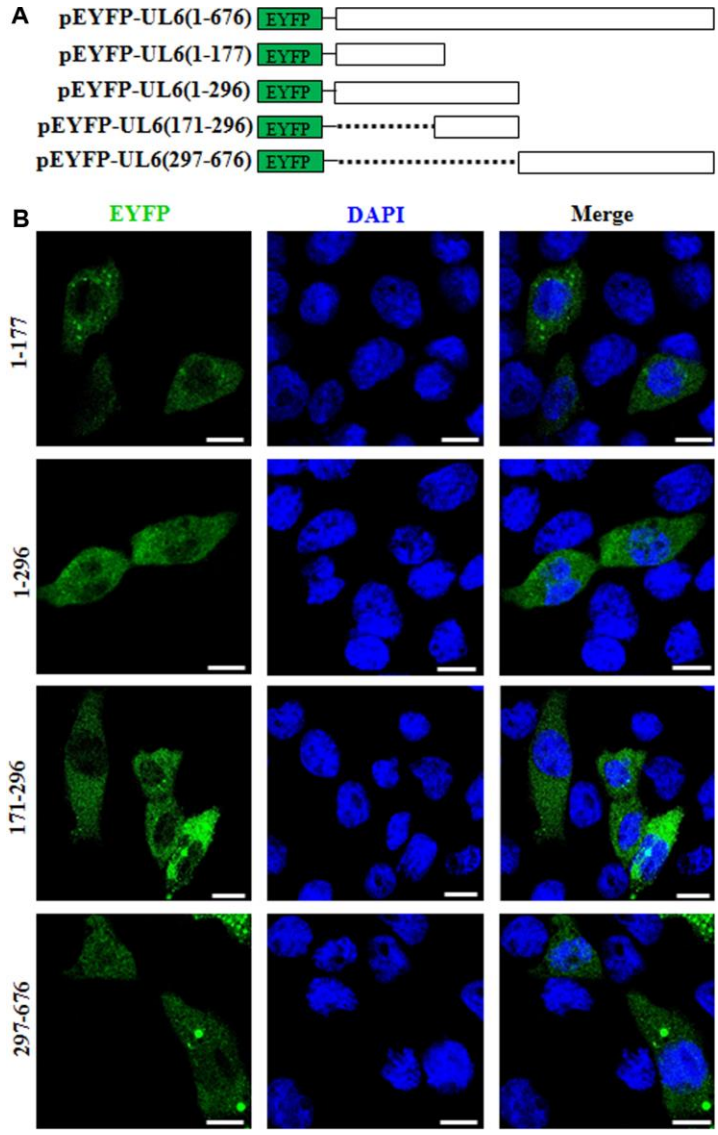

Figure 2. Subcellular distribution of the UL6 deletion mutants. (**A**) Schematic representation of wild-type UL6 protein and its N- and C-terminus deletion mutants fused with the C-terminus of EYFP. (**B**) Subcellular distribution of these UL6 deletion mutants shown in (**A**). Cells were stained with DAPI to visualize the nuclei. All scale bars indicate 10 um. Statistical analysis of the fluorescence was shown in Table 2.

Table 2. Subcellular localization of HSV-1 UL6 deletion mutants.

Transfection of UL6 deletion mutant fused with EYFP	Total number of cells transfected with plasmid	Subcellular localization pattern of transfected plasmid	Number of cells with similar subcellular localization pattern	Percentage of cells with similar subcellular localization pattern
1-296	30	Pan-cytoplasmic	28	93.33
1–177	30	Pan-cytoplasmic	27	90
171–296	30	Pan-cytoplasmic	28	93.33
297-676	30	Pan-cellular	26	86.67

COS-7 cells were transfected with plasmid expressing UL6 deletion mutants 1-296, 297-676, 1–177 and 171–296 fused to the C-terminus of EYFP. 24 h post-transfection, cells were examined by confocal fluorescence microscopy.

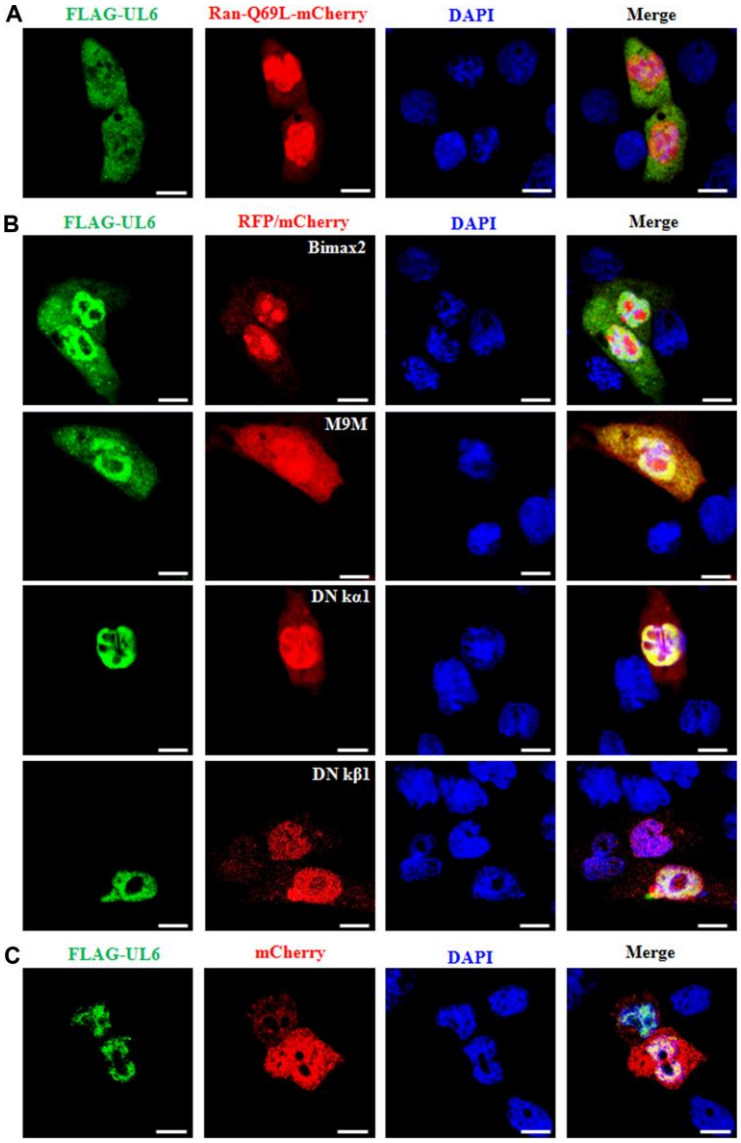

Figure 3. Nuclear import mechanism of UL6. (**A**) Fluorescence microscopy of COS-7 cells co-transfected with plasmids pFLAG-UL6 and pRan-Q69L-mCherry. (**B**) Fluorescence microscopy of COS-7 cells co-transfected with plasmid pFLAG-UL6 and plasmid encoding Bimax2-RFP, M9M-RFP, DN kα1-mCherry or DN kβ1-mCherry. (**C**) Fluorescence microscopy of COS-7 cells co-transfected with pFLAG-UL6 and pmCherry-N1. FITC-labeled proteins and mCherry fusion proteins were shown in its original color green and red, respectively, and the merged image was presented in yellow signal. All scale bars indicate 10 um, Statistical analysis of the fluorescence was shown in Table 3.

Table 3. Nuclear import mechanism of HSV-1 UL6.

Transfected viral gene	Co-transfected vector, DN mutant or inhibitor of nuclear import related receptor	Total number of cells co-transfected with two plasmids (viral gene and vector, DN mutant or inhibitor of nuclear import related receptor)	Subcellular localization change of viral gene in cells co-transfected with two plasmids	Subcellular localization pattern of viral gene in cells co-transfected with two plasmids	Number of subcellular localization change of viral gene in cells co-transfected with two plasmids	Percentage of subcellular localization change of viral gene in cells co-transfected with two plasmids
FLAG-UL6	DN Ran-mCherry	30	Yes	Pan-cellular	28	93.33
FLAG -UL6	RFP-Bimax2	30	Yes	Pan-cellular, with slightly more fluorescence in nucleus	23	76.67
FLAG -UL6	RFP-M9M	30	Yes	Pan-cellular, with slightly more fluorescence in nucleus	25	83.33
FLAG -UL6	DN kα1-mCherry	30	No	Predominantly nuclear	2	6.67
FLAG -UL6	DN kβ1-mCherry	30	No	Predominantly nuclear	1	3.33
FLAG -UL6	mCherry	30	No	Predominantly nuclear	0	0

Expression plasmid of FLAG-UL6 was co-transfected with the plasmid expressing Ran-Q69L-mCherry, RFP-Bimax2, RFP-M9M, DN kα1-mCherry, DN kβ1-mCherry or mCherry into COS-7 cells. 24 h post-transfection, cells were examined for the subcellular localization of UL6 by confocal fluorescence microscopy.

co-transfection of Bimax2 and M9M could efficiently diminished the nuclear import of UL6, whereas DN kα1 or DN kβ1 did not obviously lessened the nuclear trafficking of UL6. As negative control, UL6 was not relocalized by mCherry when COS-7 cells were co-transfected with pCMV-Flag-UL6 and mCherry vector (Figure 3C and Table 3). These data revealed that the nuclear transport of UL6 was mediated by transportin-1, and may be one of the cellular transporters of importin α1, α3, α6 and α7, but not importin α5 or importin β1.

UL6 interacts with transportin-1, importin α1 and importin α7

To further verify the assumption mentioned above, plasmids combination of pFLAG-CMV-transportin-1/pEYFP-UL6, Flag-kα2 (importin α1)/pEYFP-UL6, Flag-kα4 (importin α3)/pEYFP-UL6, Flag-kα1/pEYFP-UL6, Flag-kα6 (importin α7)/pEYFP-UL6 or pCMV9-3×Flag-importin β1/pEYFP-UL6 were co-transfected into HEK293T cells for 24 h, then cell lysates were collected and co-immunoprecipitation (Co-IP) was implemented using anti-Flag mAb or mouse IgG. As results, UL6 was efficiently Co-IPed with transportin-1 (Figure 4A), importin α1 (Figure 4B) and importin α7 (Figure 4E), but not, importin α3 (Figure 4C), importin α5 (Figure 4D) or importin β1 (Figure 4F). In contrast, no target protein was Co-IPed by IgG (Figure 4), illustrating UL6 could interact with transportin-1, importin α1 and importin α7.

Verification of the nuclear import mechanism of UL6

To finally validate the nuclear import mechanism of UL6, short hairpin RNA (shRNA) expression plasmids were constructed to knock down the expression of importin α1, importin α7 and transportin-1. Compared to the shRNA control vector (shRandom), shImportin-α1, shImportin-α7 and shTransportin-1 could effectively knock down the expression of importin α1, importin α7 and transportin-1, respectively (Figure 5A), suggesting the related shRNA expression plasmids were successfully

constructed. Then, one or two or three plasmids combination of shImportin-α1, shImportin-α7 and shTransportin-1 were co-transfected with pFLAG-UL6 into COS-7 cells and IFA was carried out to analyze whether these shRNA expression plasmids can influence the nuclear import of UL6. As results, the nuclear translocation of UL6 was not obviously affected when one of importin α1, importin α7 and transportin-1, or two of importin α1/importin α7 and importin α1/transportin-1, were knocked down. However, the nuclear trafficking of UL6 was significantly inhibited when importin α7/transportin-1 or importin α1/importin α7/transportin-1 were simultaneously knocked down (Figure 5 and Table 4), confirming UL6 could be imported into the nucleus via various transport pathways, which was primarily mediated by importin α7 and transportin-1.

As we known, HSV-1 encodes more than 80 structural proteins, some of which need to be transported into the nucleus for their functions execution, such as promoting viral proliferation, restraining host transcription and expression, inhibiting host innate immunity, etc. The nuclear accumulation of these proteins is mediated by one or more different nuclear import receptors, of course including importin α1, importin α7 and transportin-1. In addition, some host proteins also need to be transported into the nucleus by different nuclear import receptors, to perform their corresponding functions. Therefore, it is bound to affect the nuclear accumulation of many proteins of HSV-1 (and host) when the DN mutants of importin α 1, importin α 7 and transportin-1 are transfected into cells or these nuclear import receptors are knocked down by shRNA expression plasmid. Consequently, it is difficult for us to determine whether the reduction of DNA replication, nucleocapsid assembly and virions production of HSV-1 is the direct outcome of the inhibition of UL6 nuclear translocation.

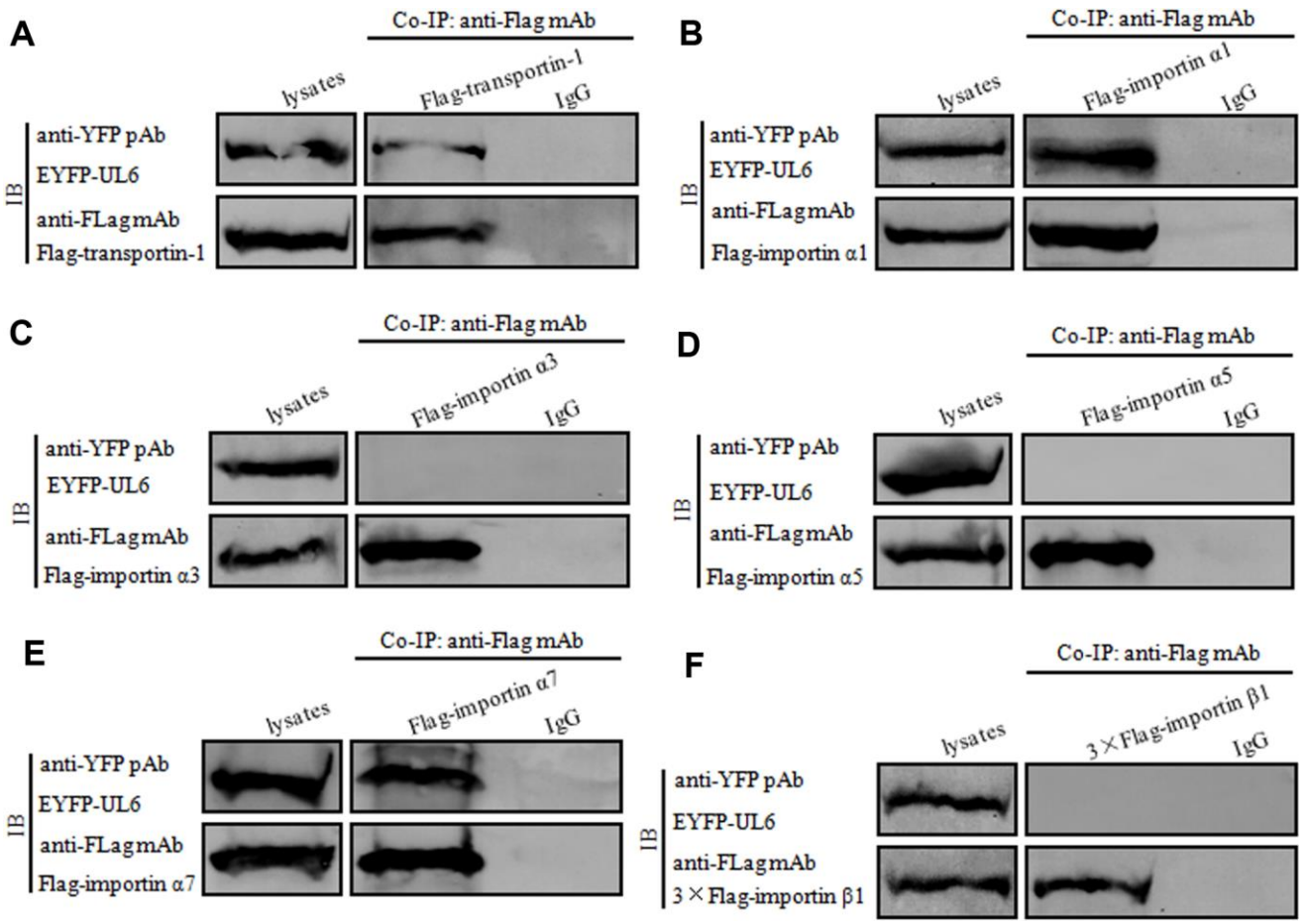

Figure 4. UL6 binds transportin-1, importin α1 and importin α7. (**A**–**F**) Co-IP of UL6 with Transportin-1 (**A**), importin α1 (**B**), importin α3 (**C**), importin α5 (**D**), importin α7 (**E**) or importin β1 (**F**). pEYFP-UL6 was co-transfected with plasmid expressing pFLAG-CMV-transportin-1 (**A**), Flag-kα2 (importin α1) (**B**), Flag-kα4 (importin α3) (**C**), Flag-kα1 (importin α5) (**D**), Flag-kα6 (importin α7) (**E**) or pCMV9-3×Flag-importin β1 (**F**) into HEK293T cells. 24 h post-transfection, cells were lysed and Co-IPed with anti-Flag mAb or mouse IgG control. Cell lysates and the Co-IPed proteins were separated in denaturing 10% SDS-PAGE, and analyzed by IB with anti-Flag mAb or anti-YFP pAb.

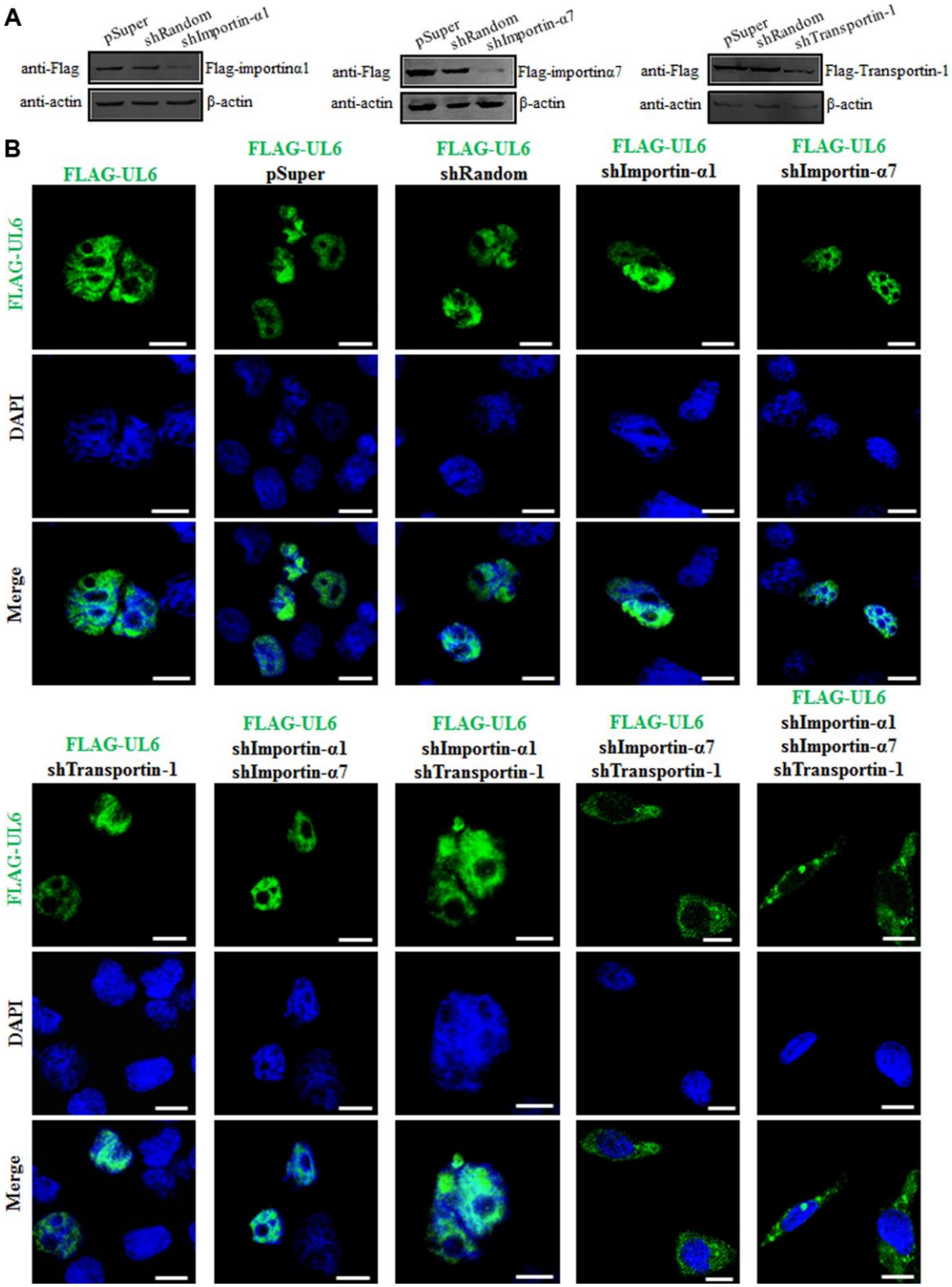

Figure 5. Subcellular distribution of UL6 in presence of different shRNA expression plasmids. (**A**) Verification of knock down efficiency of the constructed shRNA expression plasmids for importin α1, importin α7 and transportin-1. HEK293T cells were co-transfected with the plasmids combination of Flag-kα2 (importin α1)/pSuper, Flag-kα2/shRandom, Flag-kα2/shImportin-α1, Flag-kα6 (importin α7)/pSuper, Flag-kα6/shRandom, Flag-kα6/shImportin-α7, pFLAG-CMV-transportin-1/pSuper, pFLAG-CMV-transportin-1/shRandom or pFLAG-CMV-transportin-1/shTransportin-1 for 24 h. Then, cells were lysed and IB was performed with anti-Flag mAb. β-actin was used as a loading control. (**B**) One or two or three plasmids of shImportin-α1, shImportin-α7 and shTransportin-1 were co-transfected with pFLAG-UL6 into COS-7 cells for 24 h, then IFA was carried out using confocal fluorescence microscopy. Statistical analysis of the fluorescence was shown in Table 4.

Table 4. Verification of the nuclear import mechanism of HSV-1 UL6.

Transfected viral gene	Co-transfected with one or two or three plasmids of shImportin α1, shImportin α7 and shTransportin-1	Total number of cells with FLAG-UL6 fluorescence	Subcellular localization change of cells with FLAG-UL6 fluorescence	Subcellular localization pattern of cells with FLAG-UL6 fluorescence	Number of subcellular localization change of cells with FLAG-UL6 fluorescence	Percentage of subcellular localization change of cells with FLAG-UL6 fluorescence
FLAG-UL6	shVector	30	No	Predominantly nuclear	0	0
FLAG-UL6	shRandom	30	No	Predominantly nuclear	0	0
FLAG-UL6	shImportin-α1	30	No	Predominantly nuclear	1	3.33
FLAG-UL6	shImportin-α7	30	No	Predominantly nuclear	1	3.33
FLAG-UL6	shTransportin-1	30	No	Predominantly nuclear	2	6.67
FLAG-UL6	shImportin-α1+ shImportin-α7	30	No	Predominantly nuclear	3	10
FLAG-UL6	shImportin-α1+ shTransportin-1	30	No	Predominantly nuclear	3	10
FLAG-UL6	shImportin-α7+ shTransportin-1	30	Yes	Pan-cytoplasmic	26	86.67
FLAG-UL6	shImportin-α1+ shImportin-α7+shTransportin-1	30	Yes	Pan-cytoplasmic	28	93.33

shVector, shRandom, one or two or three plasmids of shImportin-α1, shImportin-α7 and shTransportin-1 were co-transfected with FLAG-UL6 into COS-7 cells. 24 h post-transfection, cells were examined for the subcellular localization of UL6 by IFA using confocal fluorescence microscopy.

In conclusion, we had proved that UL6 was a genuine nuclear localization protein. Although the predicted NLS of UL6 was nonfunctional, it was identified to be transported into the nucleus through Ran-, transportin-1-, importin α1- and importin α7-dependent nuclear import mechanism, which was largely mediated by the later two nuclear import receptor. These results dissected the molecular determinant for the nuclear transport of UL6, and will shine light for the further study of its biological roles during HSV-1 infection.

MATERIALS AND METHODS

Plasmids construction

DNA polymerase KOD-Plus-Neo, restriction enzyme and T4 DNA ligase that involved in molecular cloning were supplied by TOYOBO (Osaka, Japan), New England Biolabs (MA, USA) and Takara (Dalian, China), respectively. The UL6 ORF of HSV-1 (F strain) was amplified from plasmid template pYEbac102 [40] and inserted into pEYFP-C1 (Clontech) to yield pEYFP-UL6, as described in our previous studies [13, 15, 18, 22–24, 41]. Subsequently, the UL6 ORF of pEYFP-UL6 was subcloned into pFLAG-CMV-2 (Sigma) to produce pCMV-Flag-UL6. The deletion mutants of UL6 fused to the C-terminus of EYFP were constructed with similar method, and the related primers used for UL6 are available upon request. In addition, the shRNAs for importin α1 (5′-CTACCTCTGAAGGCTACACTT-3′), importin α7 (5′-CCTGTGTTGATCGAAATCCTT-3′), transportin-1 (5′-CCGTACTGTGAACCTGTGTAT-3′) and a control shRNA (shRandom, 5′-CTCAA CTCACGTGTCTAGTGTC-3′) were inserted into pSUPER.retro.puro (shVector) (BD Biosciences) to construct pSUPER-shImportin α1 (shImportin-α1), pSUPER-shImportin α7 (shImportin-α7), pSUPER-shTransportin-1 (shTransportin-1) and pSUPER-shRandom (shRandom), respectively.

pRan-Q69L-mCherry, pFLAG-CMV-transportin-1, pDN kα1-mCherry and pDN kβ1-mCherry were

described in our previous studies [14–19, 21, 22, 24]. Plasmids expressing RFP-M9M and RFP-Bimax2 were generously offered by Dr. Nobuyuki Nukina [42], and other plasmids were afforded as indicated by Dr. Yoshihiro Yoneda [43] (Flag-kα1 and Flag-kα6), Dr. Riku Fagerlund [44] (Flag-kα2 and Flag-kα4) and Dr. Ben Margolis (pCMV9-3×Flag-importinβ1).

Plasmid transfection and fluorescence analysis

Plasmid transfection and fluorescence analysis were carried out, as described in our previous studies [13, 15, 18, 22–24, 41, 45]. Briefly, COS-7 cells were transiently transfected with the indicated plasmid DNA mixed with Thermo Scientific TurboFect Transfection Reagent in line with the manufacturer's instructions. 24 h post-transfection, DAPI staining, which is widely applied in our previous studies of related fluorescent experiments [12–15, 17, 18, 20, 21], was employed to investigate whether the target protein locates in the nucleus or in the cytoplasm. Then, cells were analyze by live cells fluorescence microscopy or IFA, using a laser scanning confocal microscopy (Leica SP8). The image shown represents a great proportion of the cells with homogeneous subcellular distribution. EYFP fusion proteins were shown in pseudocolor green, FITC-labeled proteins and mCherry fusion proteins were shown in their original colors green and red, respectively, and the merged image was presented in yellow signal. All scale bars indicate 10 um, and images were processed using Adobe Photoshop.

Virus infection and IFA

Vero cells infected with HSV-1 (MOI=1) for 8 h were fixed with 4% paraformaldehyde, permeabilized with 0.5% Triton X-100, and stained with the anti-UL6 polyclonal antibody (pAb) [46]. Then, cells were incubated with fluorescein isothiocyanate (FITC)-conjugated goat anti-rabbit immunoglobulin G (Zymed Laboratories) and stained with DAPI. Cells were finally detected with a laser scanning confocal microscopy. All scale bars indicate 10 um, and images were processed with Adobe Photoshop.

Co-IP and immunoblotting

Co-IP and immunoblotting (IB) assays were manipulated as described previously [13, 15, 18, 22–24, 41, 47, 48]. Summarily, HEK293T cells were co-transfected with FLAG- or EYFP-tagged expression plasmids for 24 h. Cells were then collected and lysed on ice with 1 mL of lysis buffer. The lysate was subsequently incubated with anti-Flag monoclonal antibody (mAb, Sigma) or nonspecific mouse control antibody (IgG) and a 1:1 slurry of Protein A/G PLUS-Agarose (Santa Cruz Biotechnology) for at least 4 h or overnight at 4 ºC. Then, lysis buffer was used to wash beads for three times. Finally, cell lysates and the Co-IPed proteins, were subjected to IB analysis with anti-Flag mAb and anti-YFP pAb (Santa Cruz Biotechnology). All Co-IP were duplicated at least two times, and analogous data were obtained.

Abbreviations

aa: amino acids; Co-IP: Co-immunoprecipitation; DN: Dominant negative; EYFP: enhanced yellow fluorescent protein; FITC: fluorescein isothiocyanate; HSV-1: Herpes simplex virus 1; IB: immunoblotting; IFA: Immunofluorescence assay; mAb: monoclonal antibody; NLS: nuclear localization signal; NPC: nuclear pore complex; pAb: polyclonal antibody; shRNA: short hairpin RNA.

ACKNOWLEDGMENTS

We thank Drs. Yasushi Kawaguchi, Yoshinari Yasuda, Haitao Guo, Nobuyuki Nukina, Yoshihiro Yoneda, Ben Margolis, Christopher F. Basler, Donna D. Zhang, Christoph Kaether and Riku Fagerlund for the generous gifts of pYEbac102, pGEX-Ran-Q69L, DN kα1, DN kβ1, RFP-M9M/RFP-Bimax2, Flag-kα1 (importin α5), pCMV9-3×FLAG-importin β1, Flag-kα6 (importin α7), Flag-kα2 (importin α1) and Flag-kα4 (importin α3), respectively.

CONFLICTS OF INTEREST

The authors declare no conflicts of interest with the current manuscript.

FUNDING

This work was supported by grants from the National Natural Science Foundation of China (81772179); the Natural Science Foundation of Guangdong Province (2019A1515010395 and 2018A0303130257); the Regular University Distinguished Innovation Project from Education Department of Guangdong Province, China (2018KTSCX184); the Medical Scientific Research Foundation of Guangdong Province, China (B2012165); the Guangzhou Health and Medical Collaborative Innovation Program (201803040007), the Guangzhou Innovation and Entrepreneurship Leading Team Program (CYLJTD-201602); the Guangzhou Entrepreneurship Leading Talents Program (LYC201315), the Science and Technology Program of Guangzhou Development District (2018-L081); the High-Level Universities Academic Backbone Development Program of Guangzhou Medical University; the Undergraduate Laboratory Opening Project of Guangzhou Medical University (2018 and

2019); and the National, Provincial and College Training Programs of Innovation and Entrepreneur-ship for Undergraduates in Guangzhou Medical University (201910570019, S201910570088, 2018A113 and 2017A075).

REFERENCES

1. Patel AH, Rixon FJ, Cunningham C, Davison AJ. Isolation and characterization of herpes simplex virus type 1 mutants defective in the UL6 gene. Virology. 1996; 217:111–23. https://doi.org/10.1006/viro.1996.0098 PMID:8599195

2. Newcomb WW, Juhas RM, Thomsen DR, Homa FL, Burch AD, Weller SK, Brown JC. The UL6 gene product forms the portal for entry of DNA into the herpes simplex virus capsid. J Virol. 2001; 75:10923–32. https://doi.org/10.1128/JVI.75.22.10923-10932.2001 PMID:11602732

3. Wills E, Scholtes L, Baines JD. Herpes simplex virus 1 DNA packaging proteins encoded by UL6, UL15, UL17, UL28, and UL33 are located on the external surface of the viral capsid. J Virol. 2006; 80:10894–99. https://doi.org/10.1128/JVI.01364-06 PMID:16920825

4. Albright BS, Nellissery J, Szczepaniak R, Weller SK. Disulfide bond formation in the herpes simplex virus 1 UL6 protein is required for portal ring formation and genome encapsidation. J Virol. 2011; 85:8616–24. https://doi.org/10.1128/JVI.00123-11 PMID:21593161

5. Patel AH, MacLean JB. The product of the UL6 gene of herpes simplex virus type 1 is associated with virus capsids. Virology. 1995; 206:465–78. https://doi.org/10.1016/S0042-6822(95)80062-X PMID:7831802

6. Thurlow JK, Rixon FJ, Murphy M, Targett-Adams P, Hughes M, Preston VG. The herpes simplex virus type 1 DNA packaging protein UL17 is a virion protein that is present in both the capsid and the tegument compartments. J Virol. 2005; 79:150–58. https://doi.org/10.1128/JVI.79.1.150-158.2005 PMID:15596811

7. Yang K, Baines JD. Tryptophan residues in the portal protein of herpes simplex virus 1 critical to the interaction with scaffold proteins and incorporation of the portal into capsids. J Virol. 2009; 83:11726–33. https://doi.org/10.1128/JVI.01463-09 PMID:19740984

8. Yang K, Wills E, Baines JD. The putative leucine zipper of the UL6-encoded portal protein of herpes simplex virus 1 is necessary for interaction with pUL15 and pUL28 and their association with capsids. J Virol. 2009; 83:4557–64. https://doi.org/10.1128/JVI.00026-09 PMID:19224991

9. Nellissery JK, Szczepaniak R, Lamberti C, Weller SK. A putative leucine zipper within the herpes simplex virus type 1 UL6 protein is required for portal ring formation. J Virol. 2007; 81:8868–77. https://doi.org/10.1128/JVI.00739-07 PMID:17581990

10. van Zeijl M, Fairhurst J, Jones TR, Vernon SK, Morin J, LaRocque J, Feld B, O'Hara B, Bloom JD, Johann SV. Novel class of thiourea compounds that inhibit herpes simplex virus type 1 DNA cleavage and encapsidation: resistance maps to the UL6 gene. J Virol. 2000; 74:9054–61. https://doi.org/10.1128/JVI.74.19.9054-9061.2000 PMID:10982350

11. Yang K, Homa F, Baines JD. Putative terminase subunits of herpes simplex virus 1 form a complex in the cytoplasm and interact with portal protein in the nucleus. J Virol. 2007; 81:6419–33. https://doi.org/10.1128/JVI.00047-07 PMID:17392365

12. White CA, Stow ND, Patel AH, Hughes M, Preston VG. Herpes simplex virus type 1 portal protein UL6 interacts with the putative terminase subunits UL15 and UL28. J Virol. 2003; 77:6351–58. https://doi.org/10.1128/JVI.77.11.6351-6358.2003 PMID:12743292

13. Li M, Wang S, Cai M, Zheng C. Identification of nuclear and nucleolar localization signals of pseudorabies virus (PRV) early protein UL54 reveals that its nuclear targeting is required for efficient production of PRV. J Virol. 2011; 85:10239–51. https://doi.org/10.1128/JVI.05223-11 PMID:21795331

14. Li M, Wang S, Cai M, Guo H, Zheng C. Characterization of molecular determinants for nucleocytoplasmic shuttling of PRV UL54. Virology. 2011; 417:385–93. https://doi.org/10.1016/j.virol.2011.06.004 PMID:21777931

15. Cai M, Wang S, Long J, Zheng C. Probing of the nuclear import and export signals and subcellular transport mechanism of varicella-zoster virus tegument protein open reading frame 10. Med Microbiol Immunol. 2012; 201:103–11. https://doi.org/10.1007/s00430-011-0211-4 PMID:21755366

16. Cai M, Wang S, Xing J, Zheng C. Characterization of the nuclear import and export signals, and subcellular transport mechanism of varicella-zoster virus ORF9. J Gen Virol. 2011; 92:621–26.

https://doi.org/10.1099/vir.0.027029-0
PMID:21106804

17. Cai M, Jiang S, Zeng Z, Li X, Mo C, Yang Y, Chen C, Xie P, Bian Y, Wang J, Huang J, Chen D, Peng T, Li M. Probing the nuclear import signal and nuclear transport molecular determinants of PRV ICP22. Cell Biosci. 2016; 6:3.
https://doi.org/10.1186/s13578-016-0069-7
PMID:26816613

18. Cai M, Huang Z, Liao Z, Chen T, Wang P, Jiang S, Chen D, Peng T, Bian Y, Hong G, Yang H, Zeng Z, Li X, Li M. Characterization of the subcellular localization and nuclear import molecular mechanisms of herpes simplex virus 1 UL2. Biol Chem. 2017; 398:509–17.
https://doi.org/10.1515/hsz-2016-0268
PMID:27865090

19. Cai M, Si J, Li X, Zeng Z, Li M. Characterization of the nuclear import mechanisms of HSV-1 UL31. Biol Chem. 2016; 397:555–61.
https://doi.org/10.1515/hsz-2015-0299
PMID:26854290

20. Cai M, Chen D, Zeng Z, Yang H, Jiang S, Li X, Mai J, Peng T, Li M. Characterization of the nuclear import signal of herpes simplex virus 1 UL31. Arch Virol. 2016; 161:2379–85.
https://doi.org/10.1007/s00705-016-2910-z
PMID:27276975

21. Cai M, Wang P, Wang Y, Chen T, Xu Z, Zou X, Ou X, Li Y, Chen D, Peng T, Li M. Identification of the molecular determinants for nuclear import of PRV EP0. Biol Chem. 2019; 400:1385–94.
https://doi.org/10.1515/hsz-2019-0201
PMID:31120855

22. Li M, Jiang S, Mo C, Zeng Z, Li X, Chen C, Yang Y, Wang J, Huang J, Chen D, Peng T, Cai M. Identification of molecular determinants for the nuclear import of pseudorabies virus UL31. Arch Biochem Biophys. 2015; 587:12–17.
https://doi.org/10.1016/j.abb.2015.09.024
PMID:26450651

23. Li M, Jiang S, Wang J, Mo C, Zeng Z, Yang Y, Chen C, Li X, Cui W, Huang J, Peng T, Cai M. Characterization of the nuclear import and export signals of pseudorabies virus UL31. Arch Virol. 2015; 160:2591–94.
https://doi.org/10.1007/s00705-015-2527-7
PMID:26195191

24. Li M, Chen T, Zou X, Xu Z, Wang Y, Wang P, Ou X, Li Y, Chen D, Peng T, Wang Y, Cai M. Characterization of the Nucleocytoplasmic Transport Mechanisms of Epstein-Barr Virus BFLF2. Cell Physiol Biochem. 2018; 51:1500–17.
https://doi.org/10.1159/000495641 PMID:30497081

25. Lamberti C, Weller SK. The herpes simplex virus type 1 UL6 protein is essential for cleavage and packaging but not for genomic inversion. Virology. 1996; 226:403–07.
https://doi.org/10.1006/viro.1996.0668
PMID:8955060

26. Emmott E, Hiscox JA. Nucleolar targeting: the hub of the matter. EMBO Rep. 2009; 10:231–38.
https://doi.org/10.1038/embor.2009.14
PMID:19229283

27. Moore MS, Blobel G. The GTP-binding protein Ran/TC4 is required for protein import into the nucleus. Nature. 1993; 365:661–63.
https://doi.org/10.1038/365661a0
PMID:8413630

28. Palacios I, Weis K, Klebe C, Mattaj IW, Dingwall C. RAN/TC4 mutants identify a common requirement for snRNP and protein import into the nucleus. J Cell Biol. 1996; 133:485–94.
https://doi.org/10.1083/jcb.133.3.485
PMID:8636225

29. Davis LI. The nuclear pore complex. Annu Rev Biochem. 1995; 64:865–96.
https://doi.org/10.1146/annurev.bi.64.070195.004245
PMID:7574503

30. Panté N, Aebi U. Exploring nuclear pore complex structure and function in molecular detail. J Cell Sci Suppl. 1995; 19:1–11.
https://doi.org/10.1242/jcs.1995.Supplement_19.1
PMID:8655639

31. Kobe B. Autoinhibition by an internal nuclear localization signal revealed by the crystal structure of mammalian importin alpha. Nat Struct Biol. 1999; 6:388–97.
https://doi.org/10.1038/7625
PMID:10201409

32. Görlich D, Kutay U. Transport between the cell nucleus and the cytoplasm. Annu Rev Cell Dev Biol. 1999; 15:607–60.
https://doi.org/10.1146/annurev.cellbio.15.1.607
PMID:10611974

33. Goldfarb DS, Corbett AH, Mason DA, Harreman MT, Adam SA. Importin alpha: a multipurpose nuclear-transport receptor. Trends Cell Biol. 2004; 14:505–14.
https://doi.org/10.1016/j.tcb.2004.07.016
PMID:15350979

34. Ushijima R, Sakaguchi N, Kano A, Maruyama A, Miyamoto Y, Sekimoto T, Yoneda Y, Ogino K, Tachibana T. Extracellular signal-dependent nuclear import of STAT3 is mediated by various importin alphas. Biochem Biophys Res Commun. 2005; 330:880–86.
https://doi.org/10.1016/j.bbrc.2005.03.063
PMID:15809078

35. Sorokin AV, Kim ER, Ovchinnikov LP. Nucleocytoplasmic transport of proteins. Biochemistry (Mosc). 2007; 72:1439–57. https://doi.org/10.1134/S0006297907130032 PMID:18282135

36. Harel A, Forbes DJ. Importin beta: conducting a much larger cellular symphony. Mol Cell. 2004; 16:319–30. https://doi.org/10.1016/j.molcel.2004.10.026 PMID:15525506

37. Kosugi S, Hasebe M, Entani T, Takayama S, Tomita M, Yanagawa H. Design of peptide inhibitors for the importin alpha/beta nuclear import pathway by activity-based profiling. Chem Biol. 2008; 15:940–49. https://doi.org/10.1016/j.chembiol.2008.07.019 PMID:18804031

38. Cansizoglu AE, Lee BJ, Zhang ZC, Fontoura BM, Chook YM. Structure-based design of a pathway-specific nuclear import inhibitor. Nat Struct Mol Biol. 2007; 14:452–54. https://doi.org/10.1038/nsmb1229 PMID:17435768

39. Reid SP, Valmas C, Martinez O, Sanchez FM, Basler CF. Ebola virus VP24 proteins inhibit the interaction of NPI-1 subfamily karyopherin alpha proteins with activated STAT1. J Virol. 2007; 81:13469–77. https://doi.org/10.1128/JVI.01097-07 PMID:17928350

40. Tanaka M, Kagawa H, Yamanashi Y, Sata T, Kawaguchi Y. Construction of an excisable bacterial artificial chromosome containing a full-length infectious clone of herpes simplex virus type 1: viruses reconstituted from the clone exhibit wild-type properties in vitro and in vivo. J Virol. 2003; 77:1382–91. https://doi.org/10.1128/JVI.77.2.1382-1391.2003 PMID:12502854

41. Cai M, Liao Z, Chen T, Wang P, Zou X, Wang Y, Xu Z, Jiang S, Huang J, Chen D, Peng T, Hong G, Li M. Characterization of the subcellular localization of Epstein-Barr virus encoded proteins in live cells. Oncotarget. 2017; 8:70006–34. https://doi.org/10.18632/oncotarget.19549 PMID:29050259

42. Kino Y, Washizu C, Aquilanti E, Okuno M, Kurosawa M, Yamada M, Doi H, Nukina N. Intracellular localization and splicing regulation of FUS/TLS are variably affected by amyotrophic lateral sclerosis-linked mutations. Nucleic Acids Res. 2011; 39:2781–98. https://doi.org/10.1093/nar/gkq1162 PMID:21109527

43. Mizuguchi C, Moriyama T, Yoneda Y. Generation and characterization of a monoclonal antibody against importin α7/NPI-2. Hybridoma (Larchmt). 2011; 30:307–09. https://doi.org/10.1089/hyb.2011.0006 PMID:21707368

44. Fagerlund R, Melén K, Cao X, Julkunen I. NF-kappaB p52, RelB and c-Rel are transported into the nucleus via a subset of importin alpha molecules. Cell Signal. 2008; 20:1442–51. https://doi.org/10.1016/j.cellsig.2008.03.012 PMID:18462924

45. Li M, Zou X, Wang Y, Xu Z, Ou X, Li Y, Liu D, Guo Y, Deng Y, Jiang S, Li T, Shi S, Bao Y, et al. The nuclear localization signal-mediated nuclear targeting of herpes simplex virus 1 early protein UL2 is important for efficient viral production. Aging (Albany NY). 2020; 12:2921–38. https://doi.org/10.18632/aging.102786 PMID:32035424

46. Li M, Cui W, Mo C, Wang J, Zhao Z, Cai M. Cloning, expression, purification, antiserum preparation and its characteristics of the truncated UL6 protein of herpes simplex virus 1. Mol Biol Rep. 2014; 41:5997–6002. https://doi.org/10.1007/s11033-014-3477-y PMID:24973881

47. Chen T, Wang Y, Xu Z, Zou X, Wang P, Ou X, Li Y, Peng T, Chen D, Li M, Cai M. Epstein-Barr virus tegument protein BGLF2 inhibits NF-κB activity by preventing p65 Ser536 phosphorylation. FASEB J. 2019; 33:10563–76. https://doi.org/10.1096/fj.201901196RR PMID:31337264

48. Li M, Liao Z, Xu Z, Zou X, Wang Y, Peng H, Li Y, Ou X, Deng Y, Guo Y, Gan W, Peng T, Chen D, Cai M. The Interaction Mechanism Between Herpes Simplex Virus 1 Glycoprotein D and Host Antiviral Protein Viperin. Front Immunol. 2019; 10:2810. https://doi.org/10.3389/fimmu.2019.02810 PMID:31921110